Oxidation of Bio-Aldehyde and Bio-Alcohol to Carboxylic Acid by Water over Modified CuZnAl Catalysts

Yuewen Ye,[a] Bao Chen,[a] Xin Li,[a] Yue Ai,[a] Jia Sun,[b] Gang Ni,[a] Ling Qin,[a] and Tongqi Ye*[a]

A series of NiCuZnAl catalysts with various Cu/Ni molar ratios and XCuZnAl (X=Ni, Co, Mn, Mg, La) catalysts were prepared and used in the aldehyde-water shift (AWS) reaction with propanal as model compound. Although copper is the main site for AWS reaction, some additives also showed some effects on enhancing the catalytic activity to varying degrees. Mn promoted catalyst showed the highest propanal conversion of 22 % at 260 °C, much better than Co, La etc. Among the Ni promoted catalysts, NCZA-33 with Ni/(Ni + Cu) molar ratio of 33 % showed the best activity. The trend of activity happened to match the catalyst reducibility expressed by reduction peak temperature in TPR analysis, thus an MVK mechanism was suggested. Introduction of Ni decreases the proportion of Cu^0/Cu^+ in surface Cu species, thus suppressed the hydrogenation activity and decreased the selectivity of corresponding alco-hols. The carboxylic acid selectivity increased from 86.3 % of pristine CuZnAl to more than 90 % on modified catalysts, even 99.6 % on NCZA-83 catalyst. Both pristine and modified CuZnAl catalysts showed good stability under AWS reaction conditions and carbon deposition is not responsible for the deactivation. AWS reaction was also extended to other aliphatic aldehydes and alcohols, but it's invalid for furfural and Cinnamaldehyde under the employed reaction conditions. The results indicate AWS reaction is very sensitive to the nature of reactants.

Introduction

Biomass is a rich, renewable and environmentally friendly resource which can be used as an alternative feedstock for energy sources or chemicals.[1] Compare to fossil chemicals, the most important feature of bio-chemicals is they are comprised of a large amount of oxygen-containing compounds, including alcohols and aldehydes, such as ethanol, furfural, glycerol and their derivatives.[2] Those alcohols and aldehydes can be further oxidized to corresponding carboxylic acids by the oxidant of dioxygen or some soft oxidant such as H_2O, CO_2 and N_2O.[3] With increasing concerns about biomass conversion and utilization, nowadays, soft oxidation has attracted more and more attention to avoid over-oxidation by O_2. Moreover, another feature of bio-chemicals is the high moisture content in their raw product, and the moisture could be used directly to react with aldehyde to perform aldehyde-water shift (AWS) reaction (Eq. 1). When in the AWS reaction, one proton in water is to form molecular hydrogen while the hydroxyl group is incorporated into the carboxyl group.[3d] With using soft oxidants, reaction could be more gently thus selectivity of target product be enhanced. Over-oxidation to CO/CO_2 can be avoided except for steam reforming at high temperatures (Eq. 2).

$$RCHO + H_2O \rightarrow RCOOH + H_2 \quad (1)$$

$$RCHO + H_2O \rightarrow x\,H_2 + y\,CO + z\,CO_2 \quad (2)$$

Several published papers have been focused on AWS reaction catalysts in the past few years. Brewster and co-workers reported a series of half-sandwich complexes of Ir, Rh, and Ru are active for the AWS reaction of alkyl and aromatic aldehydes in homogeneous catalytic system.[4] However, the usage of noble metals and the homogeneous catalytic process are unfavourable for industrialization. Therefore, the heterogeneous catalysts for AWS reaction was also been investigated. Orozco etc. proposed the AWS reaction as a step of heptanal ketonization involved oxygen vacancies on the CeO_2 catalyst.[5] Our group reported the soft oxidation of ethanol to produce acetic acid over CuCr catalyst.[3d] The oxidation is suggested to comprise of two continuous steps, namely the AWS reaction of acetaldehyde after the dehydrogenation of ethanol. Although Cr shows a positive effect on the catalytic performance, AWS reaction is still mainly occurred on the surface Cu species. Wen etc. suggested reducible support may beneficial to Cu-based AWS catalysts.[6] Among the catalysts they explored, Cu Zn-Al and Cu/CeO_2 showed best and even better than noble metal catalysts such as Pt/CeO_2 and Au/CeO_2. More than 70 % of acetic acid selectivity at high productivity was obtained under optimized reaction conditions. The synergistic effect of Cu sites and sites from reducible oxide of CeO_2 and ZnO may play an important role in the AWS reaction. However, the role of promoters remains a matter for further research and the selectivity of acid remains to rise from the perspective of green chemistry.

CuNi-based catalysts were widely used as heterogeneous catalysts in various reactions, such as water-gas shift, hydro-

[a] *Y. Ye, B. Chen, X. Li, Y. Ai, Dr. G. Ni, Dr. L. Qin, Dr. T. Ye*
Anhui Province Key Laboratory of Advanced Catalytic Materials and Reaction Engineering, School of Chemistry and Chemical Engineering, Hefei University of Technology, Hefei, Anhui, 230009, P.R. China
E-mail: yetq@hfut.edu.cn
[b] *J. Sun*
Cardiff Catalysis Institution, Cardiff University, Cardiff, CF24 0HW, UK

deoxygenation and steam reforming.[7] In most of them, hydro-gen is included either as reactant or product. Both Cu and Ni are active elements for reactions that involve hydrogen, thus it's reasonable to expect better performance for their hybrids. AWS is such an interesting reaction that Cu is much more active than other transition metals even noble metals, and promoters may play an important role in the enhancement of activity or selectivity.[3d,6] In this paper, we describe exploration of the AWS reaction using propanal as model compound on Ni modified Cu Zn Al catalysts to make further understanding of structure-function relationships and the promoting effects of Ni.

Results and Discussion

CuZnAl catalysts with various molar ratio of Ni/(Ni + Cu) were prepared by co-precipitation method followed by the same calcine program. Figure 1A shows the XRD patterns of NiCuZnAl catalysts before calcined. Diffractions peaks of LDHs (layered double hydrotalcites) at 11.8, 23.8, 34.9, 39.4, 47.0, 60.5 and 61.9° were observed.[8] However, the nickel oxide was no good for the formation of hydrotalcite structure thus the reflection intensity decreased with the increasing of Ni/Cu molar ratio. Figure 1B showed the XRD patterns after calcined at 450 °C. The characteristic diffraction peaks in the precursors disappeared demonstrated that the hydrotalcite-like structures were completely destroyed by calcination treatment. Only some broaden diffraction peaks were observed for these samples which may come from not well-ordered tiny crystal-lites of NiO and $ZnAl_2O_4$.[8b,9] No characteristic diffraction peak of CuO was detected, which indicates good dispersion of Cu species or exists as amorphous in the catalysts. The XRD patterns of reduced and used typical NCZA-50 catalyst are also shown in the Figure 1B. As can be seen, both of them are quite similar with the fresh prepared one. This also demonstrates that these diffraction peaks have nothing to do with CuO, for the CuO can be thoroughly reduced to Cu below 300 °C as the TPR experiment revealed.

The textural properties of NiCuZnAl catalysts with different compositions were investigated and results are summarized in Table 1. The bulk contents of metals are quite close to the molar ratio of feeding nitrates, except for a slight deviation of aluminium content from expected, which might be attributed to partly dissolved in the mother liquor during co-precipitation. The doping of Ni showed a positive effect on the catalyst surface. The specific surface area increased from 42.9 to 124.2 m^2/g with the increasing of Ni content reflecting the change of structure by Ni doping. Another promoting effect is on the copper dispersion which measured by N_2O desorption method. As shown in Figure 2, with the decreasing of Cu

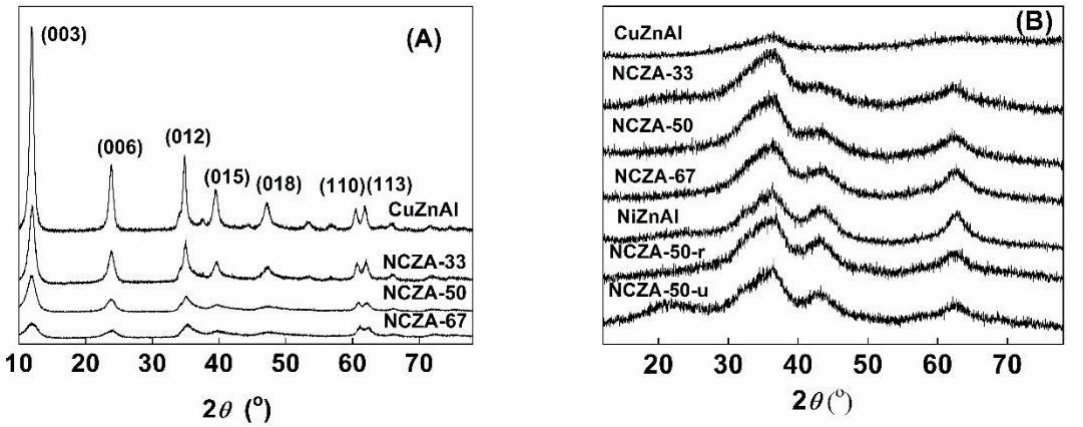

Figure 1. XRD patterns of NiCuZnAl catalysts before and after calcined (NCZA-50-r: NCZA-50 catalyst after reduced by H_2 at 300 °C for 2 h; NCZA-50-u: NCZA-50 catalyst after used at 300 °C for 5 h).

Table 1. Physico-chemical properties of the calcined mixed oxides.

Catalysts	Composition[a] (mol %)	S_{BET} (m^2 g^{-1})	PS[b] (nm)	PV[c] (cm^3 g^{-1})	Cu dispersion[d] (%)
CuZnAl	$Cu_{36}Zn_{34}Al_{30}$	42.9	14.0	0.223	16.2
NCZA-33	$Ni_{11}Cu_{25}Zn_{34}Al_{30}$	91.0	19.0	0.225	42.8
NCZA-50	$Ni_{19}Cu_{18}Zn_{33}Al_{30}$	110.2	7.45	0.228	59.2
NCZA-67	$Ni_{23}Cu_{13}Zn_{33}Al_{31}$	124.2	6.23	0.221	76.0
CoCuZnAl	$Co_{19}Cu_{18}Zn_{34}Al_{29}$	100.1	9.33	0.277	34.5
MnCuZnAl	$Mn_{19}Cu_{17}Zn_{34}Al_{30}$	110.6	28.4	0.266	55.6
MgCuZnAl	$Mg_{20}Cu_{17}Zn_{33}Al_{30}$	46.9	3.79	0.153	69.9
LaCuZnAl	$La_{19}Cu_{17}Zn_{35}Al_{29}$	47.0	10.7	0.178	34.6

[a] calculated from ICP-AES analysis; [b] average pore size; [c] average pore volume; [d] calculated by N_2O desorption.

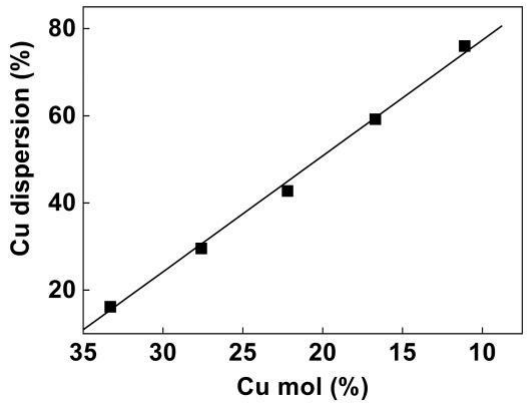

Figure 2. The relationship between Cu dispersion and content in the NiCuZnAl catalysts.

content, the Cu dispersion increased, showed an inversely proportional relation among the mixed oxides.

Figure 3A shows the H_2-reduction features of NiCuZnAl catalysts with various Ni/Cu molar ratios. The samples showed almost only one peak which could attribute to the stepwise reduction of CuO. The reduction peak was firstly shifted toward low temperature with increase of Ni doping amount, which from 275 °C of CuZnAl to 235 °C of NCZA-33. However, a further increase of Ni/(Ni + Cu) molar ratio led to the reduction peak shifted back to high temperature. This trend of change is quite similar with other works on CuNi-based hybrid oxides.[7a,10] Zhang etc. also reported 30 % Ni approximately showed the highest reducibility for the series CuNi/γ Al_2O_3 catalysts.[7b] Nevertheless, the influence of Ni-doping on CuO_x reducibility has not been studied in detail. Some researchers suggested the introduction of Ni is beneficial for the formation of NiCu alloy, which can effectively increase the reducibility of the studied samples.[11] However, in the present series catalysts, NiO_x can't be reduced to Ni^0 as illustrated below, thus the NiCu alloy can't be formed. Therefore, we prefer to ascribe it to the influence of supports. According to the published papers, the enhanced Cu reducibility by Ni-doping is usually observed on some late transition metal oxide supports such as ZnO and Fe_2O_3,[12] whereas inhibited reducibility is often observed on some early transition metal oxides such as CeO_2, ZrO_2 and TiO_2 etc.[13]

Ni species mainly exist as a mixture of Ni^{2+} and Ni^{3+} and hard to be reduced below 300 °C. As Figure 3B shows, we examined the chemical state of Ni on the surface of the typical NCZA-50 catalyst. Both the samples reduced at 300 °C for 2 h and used at 300 °C for 5 h have similar profiles with the pristine NCZA-50. The BE of Ni 2p in the reduced and used samples shifted slightly to a lower value for the partly reduction of Ni^{3+} to Ni^{2+}, however, almost no Ni^0 (main peak at about 852.6 eV) was detected.[9b,14] The poor reducibility of NiO_x species in these catalysts could attribute to the strong interactions between Ni and oxide supports namely ZnO and Al_2O_3.[15]

AWS reaction using propanal as model compound was carried out over Ni modified CuZnAl catalysts under same reaction conditions for the sake of comparison. Propionic acid is obtained as the major product along with a minor amount of propyl alcohol and a trace amount of condensation product. Results are summarized in Table 2. Under experimental conditions, CuZnAl catalyst showed 16.3 % and 22.4 % propanal conversion together with 86.3 % and 96.2 % selectivity of propionic acid for 260 and 300 °C, respectively. NiZnAl catalyst which without Cu contained is less active compared to the Cu-contained catalysts, and even no activity at the low temper-ature of 260 °C. Addition of an appropriate amount of Ni shows a great promoting effect both on catalytic activity and selectivity to propionic acid. The catalytic activity increased with the increasing of Ni/Cu ratio, while excessive Ni doping induced the decrease of activity. Among the catalysts inves-tigated, NCZA-33 with Ni/(Ni + Cu) molar ratio of 33 % showed the highest activity. Additionally, all of the Ni-promoted samples showed much better propionic acid selectivity of more than 93 % than the pristine CuZnAl catalyst of 86 % at the low

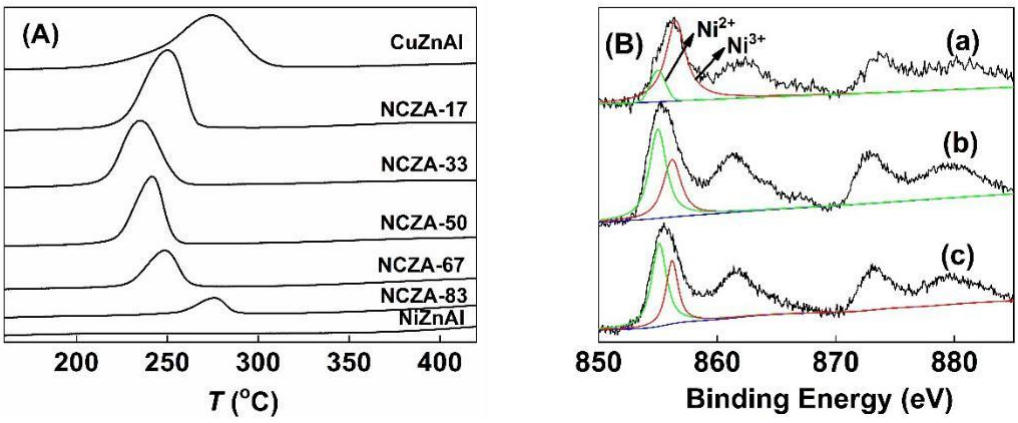

Figure 3. TPR results of NiCuZnAl catalysts (A); and Ni 2*p* XPS of NCZA-50 catalyst (B) (a: fresh prepared; b: reduced at 300 °C for 2 h; c: used at 300 °C for 5 h).

Table 2. The catalytic performance on Ni modified catalysts at 260 °C and 300 °C.

Catalysts	260 °C C (%)[a]	S_A (%)	S_B (%)	300 °C C (%)	S_A (%)	S_B (%)
CuZnAl	16.3	86.3	13.7	22.4	96.2	3.8
NCZA-17	16.7	93.6	6.4	29.3	98.0	2.0
NCZA-33	18.0	93.4	6.6	30.3	97.1	2.9
NCZA-50	16.5	93.1	6.9	26.5	97.9	2.1
NCZA-67	14.6	94.1	5.9	22.7	98.1	1.9
NCZA-83	11.7	98.4	1.6	17.3	99.6	0.4
NiZnAl	0	–	–	4.79	100	0

[a] C(%): conversion of propanal.S_A(%): selectivity of propionic acid; S_B(%): selectivity of propyl alcohol. (typical reaction conditions: 0.1 g catalyst, 0.137 g/h aldehyde or alcohol, 1.37 g/h water, 10 ml/min N_2; All products were collected between hours 2 and 3 of the reaction for GC analysis).

temperature of 260 °C. With the increasing of Ni doping amount, the propionic acid selectivity increased. The higher temperature is also beneficial to the production of propionic acid, thus the high selectivity was observed of 99.6 % at 300 °C on NCZA-83 catalyst.

As expected, the catalytic activity seems relevant to the BET surface area and Cu content to a certain extent. The interesting thing is the most active catalyst is NCZA-33, which is exactly the most reducible one in TPR experiments shown in Figure. 3 A. It seems the AWS activity more consistent with the trend of reduction peak, in other words, the reducibility of the mixed oxides.[16] To further confirm it, we prepared some other metals such as Mn, Co etc. doped CuZnAl catalysts, together with catalyst characterization and AWS reaction performed. The molar ratio of Cu : X (X=Ni, Co, Mn, Mg, La) in these catalysts are fixed at 1 : 1. The physico-chemical properties are summarized in Table 1. The BET surface area of Mg and La-doped CuZnAl is around 47 m^2/g which is very close to 42.9 m^2/g of pristine CuZnAl, while Ni, Co and Mn-doped samples showed a great increase of surface area to about 110 m^2/g. All of the modified catalysts have increased copper dispersion that from 16.2 % of CuZnAl to more than 34 %, and the highest is 69.9 % of MgCuZnAl, showed a common promoting effect of Cu segregation on the catalyst surface. These should beneficial to catalytic performance, as the surface area and copper dispersion are often considered as two important affecting factors for catalyst activity.

However, we couldn't find a strong correlation between surface area/copper dispersion and AWS activity of propanal (Figure 4). Instead, the activity seems more consistent with the TPR reduction peak temperature, just like the NiCuZnAl serials catalysts showed above. The H_2-TPR profiles of various metal-doped CuZnAl catalysts are shown in Figure 5. All the modified CuZnAl samples showed only one peak below 350 °C with relative symmetry. The doping of the fourth element increased the reducibility of bulk CuO led to the shift of reduction peak to low temperature. The Ni, Co and Mg showed a similar promoting effect of reducibility, and somewhat better than La. The great change of MnCuZnAl reducibility can be partly ascribed to the formation of spinel-like solid solution and inner

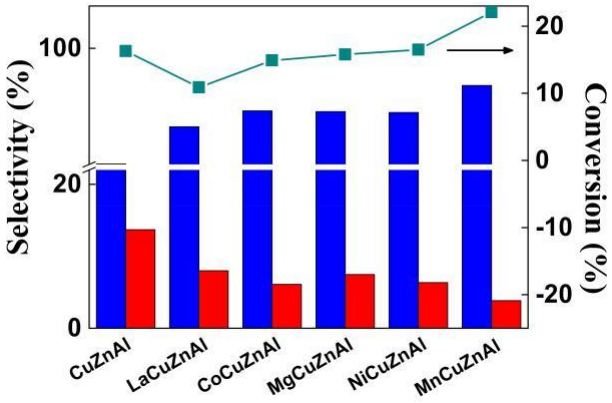

Figure 4. Propanal conversion and product selectivity over various metal doped catalysts (blue bar: selectivity of propionic acid; red bar: selectivity of propyl alcohol).

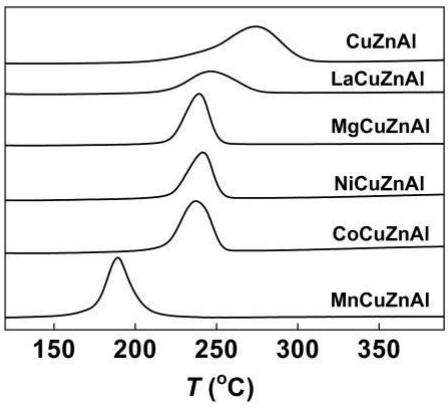

Figure 5. TPR profiles of various metal doped CuZnAl catalysts.

redox of Mn and Cu oxides,[17] that we have discussed in detail elsewhere.[18]

To illustrate the effect of the additives on catalyst reducibility and catalytic performance, the activity in propanal AWS relate to reducibility is plotted as a function of the reduction peak temperature in TPR. As can be seen from Figure 6, the activity increases with the decreasing of reduction peak, no matter for the various metals nor the Ni-doped with different Cu/Ni molar ratios.

We speculate that the redox mechanism with the oxygen species on the catalyst surface act as the oxidant might be involved in the AWS reaction. Low reduction peak in TPR represents looser Cu O bond, in which the oxygen species is more tend to leave from the oxide and react with hydrogen in TPR or with propanal in AWS reaction thus showed higher activity. The suggested Mars-van-Krevelen (MVK) mechanism is shown in Scheme 1. It is reasonable that propanal is adsorbed on the active sites and decomposed to propionyl and hydro-gen. Subsequently, the propionyl species is oxidized by lattice

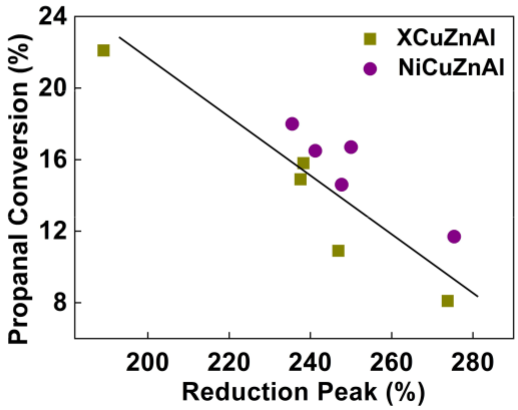

Figure 6. Total activity of the modified CuZnAl catalysts used in this work in propanal AWS at 260 °C related to the reduction peak temperature in TPR.

Table 3. Results of AWS reaction of various aldehydes and alcohols at 260 °C over NCZA-33.[a]

Substrates	Conversion (%)	Selectivity (%)		
		alcohol	aldehyde	carboxylic acid
CH3CHO	26.3	10.0	–	90.0
C2H5CHO	18.0	6.6	–	93.4
C3H7CHO	14.6	2.7	–	97.3
C2H5OH	58.5	–	90.2	9.8
C3H7OH	75.9	–	86.4	13.6
C4H9OH	83.7	–	79.0	21.0
Furfural	0.5	–	–	–
Cinnamaldehyde	–	–	–	–
1,2-propanediol	46.9	–	100[b]	–

[a] typical reaction conditions: 0.1 g catalyst, 0.137 g/h aldehyde or alcohol, 1.37 g/h water, 10 ml/min N_2; All products were collected between hours 2 and 3 of the reaction for GC analysis; [b] the only product is acet.

oxygen or hydroxyl on the catalyst surface resulting in the formation of propionic acid and the reduction of the metal oxide, which may be the rate-determining step. In order to form a cyclic redox process, the reduced copper species are then reoxidized by moisture in the feed gas.

The scope of the AWS reaction on the optimized NCZA-33 catalyst was subsequently extended to some homologues of aldehydes and alcohols and the results are summarized in Table 3. Consistent with the prior research,[3d] alcohols showed relatively high conversion but low carboxylic acid selectivity, for the intermediate product of aldehyde is more likely spread-ing to gas phase than performing in the AWS reaction. As a good hydrogenation element, Cu-based catalyst is also active in dehydrogenation, so that the alcohols showed high con-version to the corresponding aldehyde. However, the following AWS reaction is much difficult than dehydrogenation, thus the alcohol substrates showed relatively low carboxylic acid selectivity and aldehyde substrates showed lower conversion. Although dehydrogenation and hydrogenation is a pair of reversible reactions, the hydrogenation is more favourable under the current reaction conditions.[18] The dehydrogenation reaction could be severe inhibited even if under a very small partial pressure of hydrogen in the atmosphere. Similarly, the only product of 1, 2-propanediol is acetol, for the dehydrogen-ation of primary hydroxyl was suppressed by the hydrogen produced from the dehydrogenation of secondary hydroxyl. All of the aliphatic aldehydes showed high selectivity of corre-sponding carboxylic acid for more than 90 % on the optimized NCZA-33 catalyst. Along with the increasing number of carbon atoms in aliphatic aldehydes and alcohols, the selectivity of corresponding carboxylic acid selectivity increased.

When the substrate changed to some biomass derivatives such as furfural and cinnamaldehyde, almost no conversion was found. This result is quite similar with Brewster's report, although they performed the AWS reaction in homogeneous catalytic system and using Ru complexes as catalysts.[4b] The inertness of aromatic aldehyde and cinnamaldehyde in homo-

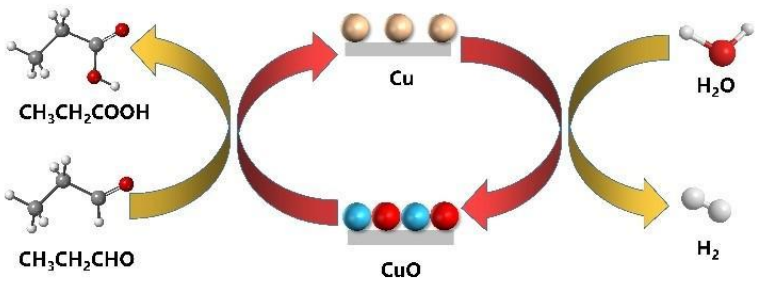

Scheme 1. Mars-van-Krevelen mechanism for AWS reaction on Cu-based catalys.

geneous AWS reaction was ascribed to their conjugate structure. The mechanism of heterogeneous AWS reaction still remains unknown. Haffad etc. proposed a Cannizzaro-like mechanism of benzaldehyde on metal oxide surface that may produce benzyl alcohol and benzoic acid.[19] However, the low reactivity of aromatic aldehyde demonstrates the Cannizzaro-like aldehyde disproportionation should be excluded under the present catalytic system. Therefore, the main by-products of alcohols should be produced by hydrogenation of corresponding aldehydes. The hydrogen comes from the product of AWS reaction, and the hydrogenation occurred on Cu sites.[20] Since alcohol is almost the only by-product, the way to enhance the selectivity of carboxylic acid should be restraining the catalytic hydrogenation activity. This can be achieved by decreasing the proportion of Cu^0/Cu^+ species on the catalyst surface, for the Cu^0/Cu^+ species are considered to be the active sites for hydrogenation reactions.[21]

To further confirm it, the chemical states of the representative Ni-doped CuZnAl catalysts after used in AWS reaction were evaluated by XPS. As Figure 7 shows, all the samples showed the Cu $2p_{3/2}$ and Cu $2p_{1/2}$ peaks at about 932.2 and 952.1 eV which were the characteristic peaks of Cu^0/Cu^+ species, together with peaks around 934.5 and 954.8 eV which could be ascribed to Cu^{2+} species.[7c] Results showed the coexistence of Cu^{2+} and Cu^0/Cu^+ on the catalyst surface for all of these series catalysts, which is a common feature of redox mechanism catalytic reactions.[22] It is also found that with the presence of nickel oxides, the stability of Cu^{2+} was enhanced and the proportion of Cu^{2+} in the total surface Cu^{2+} species had increased with the increasing of Ni doping. Thus, one can reasonably speculate that NCZA-33 happened to provide an optimum Cu^{2+} to Cu^0/Cu^+ ratio which beneficial to catalytic activity in AWS reaction. It's noteworthy that all Ni-doped samples showed better propionic acid selectivity than the pristine CuZnAl catalyst, especially at the low temperature of 260 °C. As discussed above, we ascribe it to the relatively lower Cu^0/Cu^+ contained on the surface of Ni-doped catalysts, which induced lower hydrogenation activity.

The stability experiments of the CuZnAl and Ni modified (take NCZA-33 as an example) catalysts using propanal as model compound are exhibited in Figure 8. Both of the catalysts deactivated slowly during the 120 h stability tests, which may attribute to the slight sintering of Cu active centre.[13] The NCZA-33 catalyst showed a little better than CuZnAl. As can be seen, the conversion of propanal on NCZA-33 is about 2 % higher than that of CuZnAl in the first 20 h. The selectivity of propionic acid was observed slightly increased on both catalysts with time on stream. Throughout the whole stability tests, the selectivity on NCZA-33 is about 5% higher than that of CuZnAl, showed a positive effect of Ni-doping.

To assess the impact of carbon deposition on the catalytic activity, TG analysis of used catalysts after 120 h stability tests were performed (Figure 9). For the TG profile of each catalyst, there is an increment in weight from 150 to 250 °C, which could be ascribed to the oxidization of Cu^0/Cu^+ to CuO in air

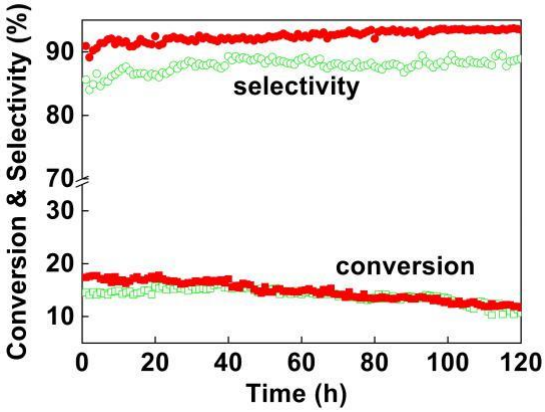

Figure 8. Long-term stability test over CuZnAl and NCZA-33 catalysts (typical reaction conditions: 0.1 g catalyst, 0.15 g/h propanal, 1.5 g/h water, 10 ml/ min N_2; green square: propanal conversion over CuZnAl, red square: conversion over NCZA-33, green circle: propionic acid selectivity over CuZnAl, red circle: selectivity over NCZA-33 catalyst).

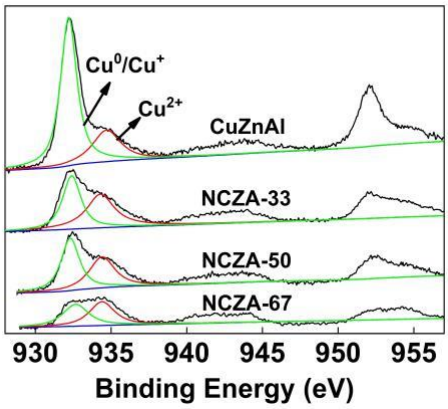

Figure 7. Cu 2p XPS spectra of the used catalysts.

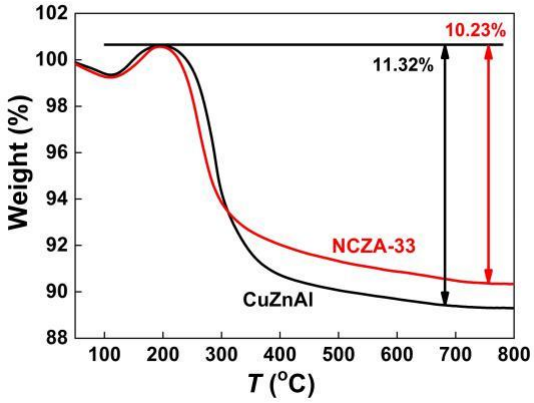

Figure 9. TG analysis of the CuZnAl and NCZA-33 catalysts after stability tests.

atmosphere. In general, the TG profiles can be divided into two different temperature regions: the first is lower than 450 °C that could be assigned to the loss of water, volatile species (such as adsorbed reactants, intermediates and products) and easily oxidizable carbonaceous species, the second region is higher than 450 °C which could be ascribed to the oxidation of deposited carbon (amorphous, filaments and graphite).[23] From the TG curves, the total weight losses are around 10 wt % for both spent catalysts. The weight loss mainly occurred in the range of below 450 °C demonstrates high content of volatile (adsorbed reactants, intermediates and products) or easily oxidizable species rather than carbon deposition. Therefore, the TG results partly explained the long-term stability of the CuZnAl-based catalysts in the AWS reaction.

Conclusion

From the results obtained in the present work, the following major conclusions were drawn:

1. The additives of fourth metal element introduced to CuZnAl catalysts modified their texture properties, especially for Ni, Co, Mn-doped samples that the specific surface area increased to more than twice that of the pristine CuZnAl catalyst.
2. Additives also enhanced reducibility of Cu species to varying degrees, which may be very good for the redox catalytic activity. The catalyst with higher reducibility in TPR showed higher activity in AWS reaction. Thus an MVK mechanism was suggested.
3. Additives with optimum amount promote the catalytic performance in both activity and selectivity. Introduction of Ni decreases the proportion of Cu^0/Cu^+ in surface Cu species, thereby, the hydrogenation activity decreased and carboxylic acid selectivity increased. More than 98 % of propionic acid selectivity was obtained at considerable conversion.
4. The AWS reaction can be extended to other aliphatic aldehydes and alcohols. However, it's showed less activity even no conversion of furfural and cinnamaldehyde under the employed reaction conditions. The results indicate AWS reaction is very sensitive to the nature of reactants. Catalysts showed very slow deactivation during the long-term stability tests. Carbon deposition is not the major cause of deactivation.

Supporting Information Summary

The supporting information includes experimental section containing materials, instruments, characterization and detailed procedure for the synthesis of catalyst.

Acknowlegements

This work was supported by the Fundamental Research Funds for the Central Universities (JZ2017HGTB0231, JZ2019HGTB0059); the National Natural Science Foundation of China (21406045); and the Natural Science Foundation of Anhui Province (1508085QB46).

Conflict of Interest

The authors declare no conflict of interest.

Keywords: Aldehyde-water shift · propanal · propanoic acid · supported catalysts · modified CuZnAl catalyst

[1] a) R. Ahorsu, F. Medina, M. Constanti, *Energies* **2018**, *11*, 19; b) P. K. Rout, A.D. Nannaware, O. Prakash, A. Kalra, R. Rajasekharan, *Chem. Eng. Sci.* **2016**, *142*, 318–346; c) U. Nda-Umar, I. Ramli, Y. Taufiq-Yap, E. Muhamad, *Catalysts* **2018**, *9*, 15.

[2] a) A. N. Marchesan, M. P. Oncken, R. Maciel Filho, M. R. Wolf Maciel, *Green Chem.* **2019**, *21*, 5168–5194; b) C. Chatterjee, F. Pong, A. Sen, *Green Chem.* **2015**, *17*, 40–71.

[3] a) Y. Wan, Z. K. Wu, H. Yu, S. Han, Y. G. Wei, *Green Chem.* **2020**, *22*, 3150–3154; b) T. Corona, A. Company, *Dalton Trans.* **2016**, *45*, 14530–14533; c) T. L. Stuchinskaya, I. V. Kozhevnikov, *Catal. Commun.* **2003**, *4*, 609– 614; d) N. Xiang, P. Xu, N. Ran, T. Ye, *RSC Adv.* **2017**, *7*, 38586–38593.

[4] a) T. P. Brewster, W. C. Ou, J. C. Tran, K. I. Goldberg, S. K. Hanson, T. R. Cundari, D. M. Heinekey, *ACS Catal.* **2014**, *4*, 3034–3038; b) T. P. Brewster, J.M. Goldberg, J. C. Tran, D. M. Heinekey, K. I. Goldberg, *ACS Catal.* **2016**, *6*, 6302–6305.

[5] L. M. Orozco, M. Renz, A. Corma, *ChemSusChem* **2016**, *9*, 2430–2442.

[6] W.-C. Wen, S. Eady, L. Thompson, *Catal. Today* **2019**. *355*,199–204.

[7] a) J.-H. Lin, P. Biswas, V. V. Guliants, S. Misture, *Appl. Catal. A* **2010**, *387*, 87–94; b) C. X. Miao, G. L. Zhou, S. Chen, H. M. Xie, X. M. Zhang, *Renewable Energy* **2020**, *153*, 1439–1454; c) T. Ye, L. Yuan, Y. Chen, T. Kan, J. Tu, X. Zhu, Y. Torimoto, M. Yamamoto, Q. Li, *Catal. Lett.* **2009**, *127*, 323–333.

[8] a) S. Velu, K. Suzuki, M. Okazaki, M. P. Kapoor, T. Osaki, F. Ohashi, *J. Catal.* **2000**, *194*, 373–384; b) C. A. Antonyraj, M. Gandhi, S. Kannan, *Ind. Eng. Chem. Res.* **2010**, *49*, 6020–6026.

[9] a) T. Rajkumar, A. Sápi, M. Abel, F. Farkas, J. F. Gómez-Pérez, A. Kukovecz, Z. Kónya, *Catal. Lett.* **2020**, *150*, 1527–1536; b) S. Velu, K. Suzuki, M. Vijayaraj, S. Barman, C. S. Gopinath, *Appl. Catal. B* **2005**, *55*, 287–299.

[10] M. d. l. A. Cangiano, M. W. Ojeda, A. C. Carreras, J. A. González, M. d. C. Ruiz, *Mater. Charact.* **2010**, *61*, 1135–1146.

[11] Z. Zhang, Q. Yang, H. Chen, K. Chen, X. Lu, P. Ouyang, J. Fu, J. G. Chen, *Green Chem.* **2018**, *20*, 197–205.

[12] a) C.-S. Chen, J.-H. You, J.-H. Lin, C.-R. Chen, K.-M. Lin, *Catal. Commun.* **2008**, *9*, 1230–1234; b) A. Jha, D.-W. Jeong, J.-O. Shim, W.-J. Jang, Y.-L. Lee, C. V. Rode, H.-S. Roh, *Catal. Sci. Technol.* **2015**, *5*, 2752–2760.

[13] a) M. M. Ambursa, T. H. Ali, H. V. Lee, P. Sudarsanam, S. K. Bhargava, S.B. A. Hamid, *Fuel* **2016**, *180*, 767–776; b) G. Ranga Rao, S. K. Meher, B.G. Mishra, P. H. K. Charan, *Catal. Today* **2012**, *198*, 140–147; c) I. Dancini-Pontes, M. DeSouza, F. A. Silva, M. H. N. O. Scaliante, C. G. Alonso, G. S. Bianchi, A. Medina Neto, G. M. Pereira, N. R. C. Fernandes-Machado, *Chem. Eng. J.* **2015**, *273*, 66–74.

[14] a) D. Srinivas, C. V. V. Satyanarayana, H. S. Potdar, P. Ratnasamy, *Appl. Catal. A* **2003**, *246*, 323–334; b) Z. Fu, J. Hu, W. Hu, S. Yang, Y. Luo, *Appl. Surf. Sci.* **2018**, *441*, 1048–1056.

[15] R. G. Kukushkin, O. A. Bulavchenko, V. V. Kaichev, V. A. Yakovlev, *Appl. Catal. B* **2015**, *163*, 531–538.

[16] G. Fierro, S. Morpurgo, M. Jacono, M. Inversi, I. Pettiti, *Appl. Catal. A* **1998**, *166*, 407–417.

[17] a) B. E. Martin, A. Petric, *J. Phys. Chem. Solids* **2007**, *68*, 2262–2270; b) F. Méndez-Martínez, F. González, E. Lima, P. Bosch, H. Pfeiffer, *J. Mex. Chem. Soc.* **2010**, *54*, 2–6; c) Y. Zhao, C. Zhao, Y. Tong, *J. Electroceram.* **2013**, *31*, 286–290.

[18] T. Q. Ye, Y. Ai, B. Chen, Y. W. Ye, J. Sun, L. Qin, X. Yao, *Catal. Commun.* **2021**. Doi 10.1016/j.catcom.**2020**.106262.

[19] D. Haffad, U. Kameswari, M. M. Bettahar, A. Chambellan, J. C. Lavalley, *J. Catal.* **1997**, *172*, 85–92.

[20] a) C. Rudolf, F. Abi-Ghaida, B. Dragoi, A. Ungureanu, A. Mehdi, E. Dumitriu, *Catal. Sci. Technol.* **2015**, *5*, 3735–3745; b) W. An, Y. Men, J. Wang, *Appl. Surf. Sci.* **2017**, *394*, 333–339.

[21] a) B. M. Nagaraja, A. H. Padmasri, B. David Raju, K. S. Rama Rao, *J. Mol. Catal. A* **2007**, *265*, 90–97; b) T.-Q. Ye, Z.-X. Zhang, Y. Xu, S.-Z. Yan, J.-F. Zhu, Y. Liu, Q.-X. Li, *Acta Phys. Chim. Sinica* **2011**, *27*. 1493–1500.

[22] a) T. Zhang, Y. Q. Hu, T. Han, Y. Q. Zhai, Y. Z. Zheng, *ACS Appl. Mater. Interfaces* **2018**, *10*, 15786–15792; b) Y. Xiao, X. D. Wu, S. Liu, J. Wan, M. Li, D. Weng, C. Q. Tong, *J. Mater. Sci.* **2016**, *51*, 5377–5387.

[23] a) M. Chen, Z. Zhou, Y. Wang, T. Liang, X. Li, Z. Yang, M. Chen, J. Wang, *Int. J. Hydrogen Energy* **2018**, *43*, 20451–20464; b) Q. L. Yang, A. Cao, N. Kang, K. An, Z. T. Liu, Y. Liu, *Fuel Process. Technol.* **2018**, *179*, 42–52.